

Suppression of *in Vivo* β -Amyloid Peptide Toxicity by Overexpression of the HSP-16.2 Small Chaperone Protein*

Received for publication, April 20, 2007, and in revised form, November 7, 2007 Published, JBC Papers in Press, November 9, 2007, DOI 10.1074/jbc.M703339200

Virginia Fonte, D. Randal Kipp, John Yerg III, David Merin, Margaret Forrestal, Eileen Wagner, Christine M. Roberts, and Christopher D. Link¹

From the Institute for Behavioral Genetics, University of Colorado, Boulder, Colorado 80309

Expression of the human β -amyloid peptide (A β) in a transgenic *Caenorhabditis elegans* Alzheimer disease model leads to the induction of HSP-16 proteins, a family of small heat shock-inducible proteins homologous to vertebrate α B crystallin. These proteins also co-localize and co-immunoprecipitate with A β in this model (Fonte, V., Kapulkin, V., Taft, A., Fluett, A., Friedman, D., and Link, C. D. (2002) *Proc. Natl. Acad. Sci. U. S. A.* 99, 9439–9444). To investigate the molecular basis and biological function of this interaction between HSP-16 and A β , we generated transgenic *C. elegans* animals with high level, constitutive expression of HSP-16.2. We find that constitutive expression of wild type, but not mutant, HSP-16.2 partially suppresses A β toxicity. Wild type A β -(1–42), but not A β single chain dimer, was observed to become sequestered in HSP-16.2-containing inclusions, indicating a conformation-dependent interaction between HSP-16.2 and A β *in vivo*. Constitutive expression of HSP-16.2 could reduce amyloid fibril formation, but it did not reduce the overall accumulation of A β peptide or alter the pattern of the predominant oligomeric species. Studies with recombinant HSP-16.2 demonstrated that HSP-16.2 can bind directly to A β *in vitro*, with a preferential affinity for oligomeric A β species. This interaction between A β and HSP-16.2 also influences the formation of A β oligomers in *in vitro* assays. These studies are consistent with a model in which small chaperone proteins reduce A β toxicity by interacting directly with the A β peptide and altering its oligomerization pathways, thereby reducing the formation of a minor toxic species.

Accumulation of the β -amyloid (A β)² peptide in the brain has been proposed to be causally linked to Alzheimer disease (the “Amyloid Cascade” hypothesis (1)), even though the specific mechanisms by which the A β peptide induces AD pathology have not been resolved. Intracellular A β accumulation has also been proposed to underlie the muscle pathology observed

in inclusion body myositis (2). To investigate A β toxicity in a genetically tractable model, we have engineered *Caenorhabditis elegans* nematodes to express the human A β -(1–42) peptide in either body wall muscle (3) or neurons (4).

In *C. elegans* transgenic models with muscle expression of A β , the peptide accumulates in intracellular cytoplasmic deposits (5) despite the inclusion of a signal peptide in the transgene construct. The appropriate removal of the signal peptide and the association of Abeta with *hsp-3*, an ER chaperone homologous to mammalian GRP78/BiP (6), have led us to propose that Abeta is routed to the secretory pathway in this model but is retrotranslocated out of the ER because it is recognized as an abnormal protein (4). We have also demonstrated a role for autophagosomes and lysosomes in the clearance of Abeta in this model, suggesting that Abeta may also exist in these subcellular compartments (8). Intracellular Abeta is observed in the muscles of IBM patients or in transgenic mouse models of IBM (9, 10), although the subcellular distribution of Abeta has not been determined. Intracellular A β has also been observed in human brain neurons (11), and the relevance of intracellular A β in Alzheimer disease has been supported by studies with the LaFerla 3 \times transgenic AD mouse model, where accumulation of intracellular A β precedes neurofibrillary tangle formation (12). A number of neurodegenerative diseases (Parkinson, Huntington, amyotrophic lateral sclerosis, etc.) are characterized by intracellular cytoplasmic accumulation of proteins causally associated with these diseases, and thus the *C. elegans* transgenic model described in this study may be generally relevant to the proteotoxicity underlying neurodegenerative diseases. In this context, a transgenic *C. elegans* strain expressing human A β has been used recently to investigate the roles of insulin-like signaling and heat shock factor in proteotoxicity (13).

A robust finding in these transgenic *C. elegans* models is the induction of the HSP-16 family of small chaperone proteins by A β expression (14, 15). HSP-16 proteins readily co-immunoprecipitate with A β in transgenic *C. elegans* worms and closely associate with intracellular A β deposits as observed by immunohistochemistry (16). The HSP-16 family proteins are homologous to α B crystallin and have been shown to have ATP-independent chaperone activity *in vitro* (17). These observations suggest that induction of HSP-16 expression by A β represents a protective response to the accumulation of an abnormal protein. This protective response could presumably alter A β toxicity by promoting A β sequestration, degradation, or refolding. Alternatively, the A β /HSP-16 interaction might alter A β multimerization, leading to a reduction in specific oligomeric or

* This work was supported by NIA Grants AG12423 and AG21037 from the National Institutes of Health (to C. D. L.). The costs of publication of this article were defrayed in part by the payment of page charges. This article must therefore be hereby marked “advertisement” in accordance with 18 U.S.C. Section 1734 solely to indicate this fact.

¹ To whom correspondence should be addressed: Institute for Behavioral Genetics/Integrative Physiology, University of Colorado, Campus Box 447, Boulder, CO 80309. Fax: 303-492-8063; E-mail: linkc@colorado.edu.

² The abbreviations used are: A β , β -amyloid peptide; AD, Alzheimer disease; ER, endoplasmic reticulum; BSA, bovine serum albumin; WT, wild type; PBS, phosphate-buffered saline; BisTris, 2-[bis(2-hydroxyethyl)amino]-2-(hydroxymethyl)propane-1,3-diol; IBM, inclusion body myositis; sHSP, small heat shock protein; GFP, green fluorescent protein.

amyloidic toxic species. Here we investigate the putative protective role of HSP-16 by examining the effect of constitutive overexpression of HSP-16 on A β toxicity and metabolism *in vivo*.

Our observations of the HSP-16 response to and interaction with A β in transgenic *C. elegans* models parallel observations made for the α B crystallin family proteins in Alzheimer brain. Ten genes have been identified in the human genome that encode small, α B crystallin-homologous proteins (18), five of which have been reported to have altered expression in AD brains. (To avoid nomenclature confusion, we will refer to these proteins using their unique HUGO identification.) Initial studies demonstrated increased immunoreactivity for CRYAB (α B crystallin) and HSPB1 (Hsp27/28) (19, 20) in AD brains. CRYAB has also been demonstrated to be increased in the temporal cortex of AD brain by mass spectrometry (21), and has been observed by immunoelectron microscopy to co-localize with A β in lens tissue from AD patients (22). Quantitative reverse transcription-PCR has also been used to demonstrate increased accumulation of CRYAB mRNA in select regions of postmortem AD brains (15). CRYAB immunoreactivity is also significantly increased in pathological muscle tissue from patients with IBM, which is characterized by intracellular A β deposition (23). More recent immunohistochemical studies have found HSPB1, HSPB6 (Hsp20), HSPB2, and HSPB8 (Hsp22) associated with senile plaques (24, 25).

Although α B crystallin-homologous small heat shock proteins (sHSP) have been found reproducibly associated with deposits of A β (and other abnormal proteins), the biological relevance of this association is unclear. Studies examining the interaction of sHSPs with A β *in vitro* have produced inconsistent, and sometimes contradictory, results. Stege *et al.* (26) reported that co-incubation of A β -(1–40) with CRYAB resulted in a decrease in fibril formation and an increase in toxicity to hippocampal neurons. Liang (27), however, observed a dose-dependent increase in thioflavin T fluorescence (typically associated with increased amyloid fibril formation) when CRYAB was incubated with A β -(1–40). A more recent study found incubation of CRYAB with either A β -(1–40) or A β -(1–42) reduced fibril formation (28). Incubation of A β -(1–40) with either CRYAA (α A-crystallin) or a functional peptide derived from α A-crystallin (mini- α A-crystallin) inhibited both fibril formation and A β toxicity to PC12 cells (29). Similarly, co-incubation of an α B-crystallin-homologous protein from the protozoan parasite *Babesia bovis* with A β -(1–40) inhibited both fibril formation and toxicity to PC12 and SY5Y cells (30). HSPB1 was reported to inhibit *in vitro* amyloidogenesis of A β -(1–42) (31), whereas a more recent study (25) failed to find an effect of HSPB8 on A β -(1–42) β -sheet formation or toxicity to human brain pericytes (although HSPB8 did inhibit β -sheet formation and toxicity of an A β -(1–40) peptide containing the Q22E substitution associated with hereditary cerebral hemorrhage with amyloidosis of the Dutch type).

The variance in the results described above may stem from the different sHSPs, A β peptides, and assays employed. However, none of these studies examined the effects of sHSP/A β interactions *in vivo*, which would address the biological relevance of this interaction more directly. We have therefore used

transgenic co-expression of A β -(1–42) and HSP-16 in a well studied *C. elegans* model to investigate the biological effects of the interaction of these proteins in a living animal. We show for the first time that a small heat shock protein can suppress A β toxicity *in vivo*.

EXPERIMENTAL PROCEDURES

Transgenic Constructions—The HSP-16.2 coding region was recovered from genomic *C. elegans* DNA by PCR, using a forward primer tagged with a 5' KpnI site, and a reverse primer tagged with a 5' EcoRI site. The PCR fragment was cleaved with KpnI and EcoRI and then inserted between the KpnI and EcoRI sites of myo-3/GFP expression vector pPD118.20, replacing the GFP coding sequence with HSP-16.2. The resulting plasmid, pCL137, was subjected to *in vitro* mutagenesis (Stratagene QuickChange kit) to generate a myo-3/HSP-16.2 R94G plasmid (pCL187). A parallel *in vitro* mutagenesis was also performed to introduce the R94G mutation into the HSP-16.2 *Escherichia coli* expression construct described previously by Leroux *et al.* (17). The pCL137 and pCL187 plasmids were independently co-injected along with marker plasmid pCL26 (mtl-2/GFP), which produces strong intestinal GFP expression. Heritable extrachromosomal lines were obtained by screening for GFP fluorescence. A completely stable chromosomally integrated strain, CL2392, was derived from extrachromosomal myo-3/HSP-16.2 strain CL1392 by γ -irradiation as described previously (3).

Paralysis Scoring—Synchronous populations of transgenic animals were generated by limited egg lay at 16 °C, and worms were allowed to develop for 48 h, thus reaching the third larval stage (L3). The worms were then upshifted to 25 °C and then scored for paralysis, typically starting 24 h after upshift. Animals were scored as paralyzed if they failed to propagate a full sinusoidal contraction after prodding, or if they were associated with a “halo” of ingested bacterial lawn, indicative of an inability to move to access food. In experiments measuring paralysis in extrachromosomal transgenic strains, sibling worms containing the transgene were identified by GFP fluorescence of the marker transgene included in the transgenic array. Identification of transgenic and nontransgenic worms was performed after paralysis scoring to prevent observer bias.

Immunoblotting and Immunohistochemistry—For immunoblot analysis, fourth larval stage nematode populations were harvested, washed free of *E. coli* by low speed centrifugation, and immediately flash-frozen in liquid nitrogen in the presence of protease inhibitors (Sigma protease inhibitor mixture, P2714). Frozen samples were solubilized by boiling 5 min in Laemmli sample buffer, and protein concentrations were determined by a modified Bradford assay using Coomassie Plus-200 reagent (Pierce) per the manufacturer's description. Protein samples were fractionated by SDS-PAGE using 4–12% acrylamide NuPAGE BisTris gels (Invitrogen) and transferred to Nybond ECL nitrocellulose membranes (Amersham Biosciences). Blots were probed with anti-HSP-16.2 antisera (gift of Peter Candido) at 1:10,000 dilution, anti-A β monoclonal 6E10 (Abcam, ab10146) at 0.7 μ g/ml, or anti-actin monoclonal JLA20 (Developmental Studies Hybridoma Bank, University of Iowa) at 1:100 dilution, and horseradish peroxidase-conjugated

secondary antibodies. ECL (Amersham Biosciences) was used for signal detection.

For immunofluorescence, nematode populations were fixed in 4% paraformaldehyde and permeabilized using collagenase/ β -mercaptoethanol treatment as described previously (3). Anti-HSP-16.2 antisera was used at 1:1000 dilution, and 6E10 was used at 10 μ g/ml. Secondary antibodies fluorescently labeled with Alexa dyes (Molecular Probes) were used at 20 μ g/ml. Images were acquired using a Zeiss Axiophot epifluorescence microscope equipped with a digital deconvolution retrofit and Slidebook analysis software (Intelligent Imaging Innovations).

For quantification of β -amyloid, live adult transgenic worms were stained with the fluorescent amyloid dye X-34 as described previously (5), and amyloid deposits were imaged under shortwave illumination after destaining. Projection images of optical sections of each stained worm were generated to capture whole body amyloid signal. To exclude the effects of background staining (see Fig. 5B), deposits were first identified by inspection, and then the masking and measurement functions of Slidebook were used to generate measurements of total amyloid signal per anterior region of each worm.

Electron Microscopy—Nematodes were prepared for observation in the electron microscope as published previously (32). Briefly, fourth larval stage animals were flash-frozen in a high pressure freezer (Balzers HPM 010) according to the technique of Dahl and Staehelin (33), in which the samples are freeze-substituted with 2% osmium tetroxide and 0.05% uranyl acetate in acetone at -80°C for 5 days, gradually warmed to room temperature, infiltrated with Araldite/Embed-812 (Electron Microscopy Sciences), and polymerized. Thin sections were stained with 2% uranyl acetate and Reynold's lead citrate. The body wall muscles of at least eight animals in each category were imaged at 80 kV on a Phillips CM10 electron microscope.

Biochemical Procedures—Recombinant His₆-HSP-16.2 fusion protein was purified from a previously described BL21(DE3) *E. coli* strain containing a pRSET A expression vector in which the *hsp-16.2* coding sequence was cloned downstream of a 4-kDa polyhistidine tag, resulting in an easily purified protein active in *in vitro* chaperone assays (17). Induced cell lysates were run through Polyprep columns (Bio-Rad) packed with nickel-Sepharose 6 Fast Flow resin (Amersham Biosciences), and captured His₆-HSP-16.2 was eluted with phosphate-buffered saline (PBS) containing 500 mM imidazole and 0.05% Triton X-100. Appropriate fractions were dialyzed against PBS containing 0.2% Triton X-100 and 20% glycerol. His₆-HSP-16.2 protein preparations were subsequently biotinylated using an EZ Link Sulfo-NHS-biotinylation kit (Pierce) per the manufacturer's instruction.

Oligomerized A β -(1–42) was prepared as described by Barghorn *et al.* (34). Lyophilized 50- μ g aliquots of A β -(1–42) (Sigma) were solubilized in 10 μ l of hexafluoro-2-propanol and incubated at 37°C for 90 min to remove secondary structure. After removal of hexafluoro-2-propanol by evaporation, A β precipitates were first resuspended in 2.2 μ l of dimethyl sulfoxide (Me₂SO) leading to an initial concentration of 5 mM peptide and then diluted to 400 μ M peptide with PBS containing 0.2% SDS. The resuspended peptide was incubated for 6 h at 37°C ,

diluted 3-fold with distilled water, then incubated an additional 18 h at 37°C . This incubation resulted in the formation of soluble A β oligomers in the 38–48-kDa range.

For HSP-16.2 pulldown reactions, 5 μ g of biotinylated HSP-16.2 was rocked with A β oligomer preparations in 1 ml of PBS + 0.02% Triton X-100 at 4°C for 30 min. To capture HSP-16.2-A β complexes, 10 μ l of streptavidin-agarose beads (pre-washed in PBS/Triton X-100 buffer) were added to the binding reaction, and the reaction was rocked for another 30 min at 4°C . The streptavidin-agarose beads were subsequently recovered by low speed centrifugation and washed extensively with cold PBS containing 0.02% Triton X-100. For immunoblot analysis, bead pellets were solubilized in sample buffer, and bound proteins were fractionated as described above.

RESULTS

The HSP-16 family in *C. elegans* consists of four closely related proteins (HSP-16.1, 16.2, 16.41, and 16.48) encoded by six genes. (There are 14 other more divergent α B-crystallin homologs in the *C. elegans* genome.) As it is not known if any of the HSP-16 proteins have specialized functions, we chose to engineer overexpression of HSP-16.2, which has been the most-studied member of the HSP-16 family. To engineer high level, constitutive HSP-16.2 expression, a genomic fragment containing the *hsp-16.2* coding region (including its single intron) was fused to the promoter of the *myo-3* gene, which encodes a myosin protein expressed specifically in body wall muscle cells. The chimeric *myo-3*/HSP-16.2 construct, along with a marker transgene, was introduced into wild type *C. elegans* strains by microinjection. To control for nonspecific transgene effects, we sought to generate a control transgene in parallel containing a single missense mutation predicted to interfere with HSP-16.2 chaperone function. Given that there are no known natural mutations in HSP-16.2, we engineered an R94G substitution, which is equivalent to the R120G mutation in α B crystallin that is associated with desmin myopathy (see Fig. 1A). The R120G mutation has been shown to reduce *in vitro* α B-crystallin chaperone activity (35, 36).

The wild type and mutant *myo-3*/HSP-16.2 transgenes were introduced by genetic mating into strain CL4176, which has been engineered to have temperature-inducible expression of *myo-3*-driven human A β -(1–42) (15). Temperature upshift of CL4176 third larval stage animals results in induction of A β expression and an irreversible paralysis that begins ~ 24 h after upshift. As shown in Fig. 1B, CL4176 worms containing the *myo-3*/HSP-16.2 transgene show significantly delayed paralysis, whereas the *myo-3*/HSP-16.2 R94G transgene has minimal effects on the time of paralysis (Fig. 1C). This experiment takes advantage of the meiotic instability of the extrachromosomal *myo-3*/HSP-16.2 transgenes, which results in populations of sibling transgenic and nontransgenic animals, allowing phenotypic comparisons of these genotypes under identical conditions. These results demonstrate that HSP-16.2 can partially counter A β toxicity and that this effect requires the wild type chaperone activity of HSP-16.2.

To investigate the biochemical effects of HSP-16.2 overexpression, the *myo-3*/HSP-16.2 transgene was chromosomally integrated by γ -irradiation, yielding a completely stable trans-

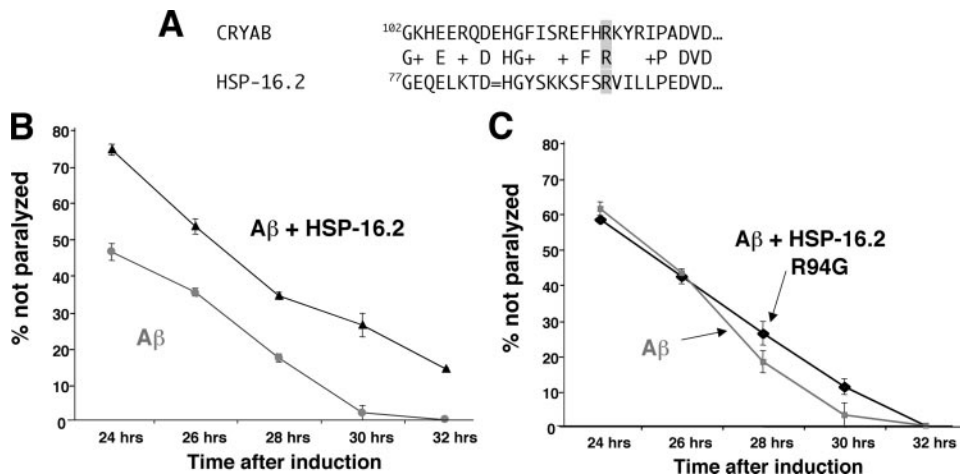


FIGURE 1. Suppression of A β toxicity by overexpression of HSP-16.2. *A*, alignment of a section of the A β crystallin domain of HSP-16.2 with human A β crystallin (CRYAB). There is 57% sequence identity in this region, including the highly conserved arginine (gray box, corresponding to positions 120 in CRYAB and 94 in HSP-16.2) that is required for full chaperone activity of CRYAB and is mutated (R120G) in desmin-related cardiomyopathy. *B*, overexpression of wild type HSP-16 significantly delays onset of A β -induced paralysis. (Black triangles, HSP-16.2 transgene-containing worms; gray squares, sibling worms that have lost the HSP-16.2 transgene.) *C*, overexpression of HSP-16.2 R94G has minimal effects on A β -induced paralysis. (Black diamonds, HSP-16.2 R94G transgene-containing worms; gray circles, sibling worms that have lost the HSP-16.2 R94G transgene.)

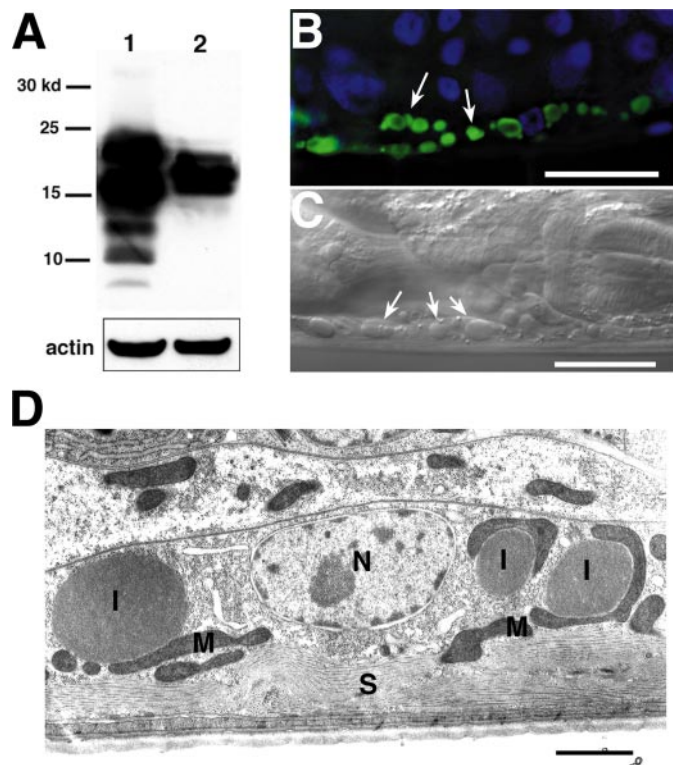


FIGURE 2. Overexpressed HSP-16.2 forms intramuscular inclusions. *A*, immunoblot of total protein from CL2392 (*myo-3*/HSP-16.2) and induced CL4176 (*myo-3*/A β) probed with polyclonal antisera raised against an HSP-16.2-specific peptide. Note significantly higher expression of HSP-16.2 protein in CL2392 in comparison to the amounts of endogenous HSP-16.2 induced by A β expression. *B*, immunohistochemical staining of CL2392 with anti-HSP-16.2 antisera reveals large immunoreactive inclusions in body wall muscles (arrows). Blue, nuclei stained with 4',6-diamidino-2-phenylindole; green, anti-HSP-16.2 immunoreactivity, bar = 20 μ m. *C*, HSP-16.2 inclusions visualized by differential interference contrast microscopy in living HSP-16.2 worms (arrows), bar = 20 μ m. *D*, electron micrograph of a body wall muscle from fourth larval stage CL2392 worm. Note electron dense inclusions not limited by a membrane. N, nucleus; S, sarcomere; I, inclusion; M, mitochondria; bar = 1 μ m.

genic strain, CL2392. Immunoblots confirmed that this strain overexpressed HSP-16.2 in comparison with the maximal level of HSP-16.2 induced by A β expression alone in strain CL4176 (Fig. 2A). Unexpectedly, overexpressed HSP-16.2 was observed to form inclusions in body wall muscle. These were visible by immunohistochemistry (Fig. 2B) and differential interference contrast light microscopy of living animals (Fig. 2C). High pressure freeze electron microscopy demonstrated that the electron-dense HSP-16.2 inclusions were not membrane-bound (Fig. 2D). Although the HSP-16.2 inclusions were commonly found in CL2392 muscle cells, no obvious effect was observed on the motility of these worms. Inclusions were also readily observable by differential interference contrast

microscopy in multiple extrachromosomal *myo-3*/HSP-16.2 lines, thereby ruling out transgene insertion into the chromosome as the cause of inclusion formation.

CL2392 (integrated *myo-3*/HSP-16.2) was crossed to three independent inducible *myo-3*/A β -(1–42) lines, and the resulting dual transgenic lines were assayed for paralysis. For all dual transgenic lines, the presence of the *myo-3*/HSP-16.2 transgenes significantly reduced paralysis onset, producing a stronger effect than that observed for the extrachromosomal *myo-3*/HSP-16.2 transgene (likely because of nonmosaic expression of the integrated transgene; see representative plot in Fig. 3A). To determine whether this suppression of paralysis rates was associated with a decrease in accumulation of A β in the dual transgenic strains, A β levels in the single and dual transgenic lines were assayed by immunoblot (Fig. 3B). Worms were harvested at 24 h after A β transgene induction, a time point when there was significantly less paralysis in the dual transgenic strains. Nevertheless, no differences were observed in either monomeric or oligomeric species detected with the anti-A β monoclonal antibody 6E10 on immunoblots. This result indicates that HSP-16.2 does not promote degradation of A β and rules out nonspecific effects on transcription of the A β transgenes by the *myo-3*/HSP-16.2 transgene (e.g. because of competition for *myo-3* transcription factors).

If HSP-16.2 does not affect A β levels, might it alter the cellular distribution of A β ? To investigate this possibility, dual transgenic lines were examined by immunohistochemistry, probing fixed worms with primary antibodies specific for A β and HSP-16. Intramuscular A β deposits were dramatically redistributed into the HSP-16.2 inclusions (Fig. 4A). To examine the specificity of this apparent sequestration of A β into the HSP-16.2 inclusions, we generated another dual transgenic strain, which contained the *myo-3*/HSP-16.2 transgene and an inducible *myo-3*/A β single chain dimer construct. Unlike A β -(1–42), the A β single chain dimer does not form amyloid

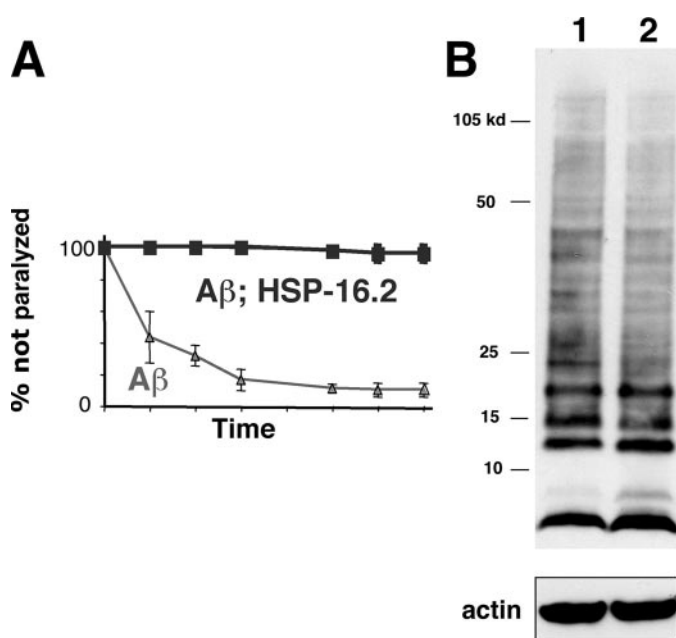


FIGURE 3. HSP-16.2 overexpression suppresses paralysis without altering A β accumulation. *A*, genetic introduction of integrated *myo-3/HSP-16* transgene from CL2393 into inducible *myo-3/A β* background dramatically delays the onset of paralysis. *B*, anti-A β immunoblot (mAb 6E10) of total protein from single transgenic (inducible *myo-3/A β* , lane 1) and dual transgenic (inducible *myo-3/A β* ; *myo-3/HSP-16.2*, lane 2) worms prepared 24 h after A β expression induction. Note very similar levels of monomeric and multimeric A β species in these two strains.

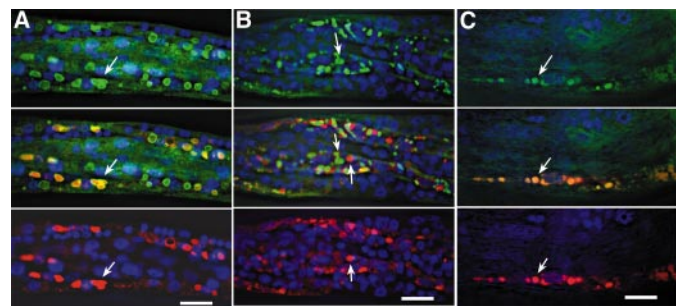


FIGURE 4. Wild type A β is sequestered into HSP-16.2 inclusions. Immunohistochemistry of dual transgenic worms with induced A β expression probed simultaneously with anti-HSP-16.2 antisera (green, upper panels) and anti-A β mAb 6E10 (red, lower panel). Blue is nuclear counterstaining with 4',6-diamidino-2-phenylindole, and middle panels are fused images, size bars = 20 μ m. *A*, inducible *myo-3/A β* ; *myo-3/HSP-16.2* worm. Note tight co-localization of A β and HSP-16.2 immunoreactivity (arrows). *B*, inducible *myo-3/A β* single chain dimer; *myo-3/HSP-16.2* worm. Note lack of association between HSP-16.2 and A β immunoreactivity (arrows). *C*, inducible *myo-3/A β* ; *myo-3/HSP-16.2* R94G. Note A β immunoreactivity also co-localizes with R94G mutants HSP-16.2 inclusions (arrows).

fibrils when constitutively expressed (37) and does not strongly associate with endogenous HSP-16 (16). As shown in Fig. 4*B*, induced A β single chain dimer does not redistribute into the HSP-16.2 inclusions, arguing that the redistribution of A β into the inclusions is because of a specific interaction between HSP-16.2 and A β , rather than a nonspecific co-aggregation. However, the sequestration of A β into the HSP-16.2 inclusions is also observed in animals expressing HSP-16.2 R94G (Fig. 4*C*), suggesting that sequestration *per se* may not be the mechanism of HSP-16.2 suppression of A β toxicity.

Although HSP-16.2 did not appear to alter overall levels of A β , it might alter folding or multimerization pathways, altering

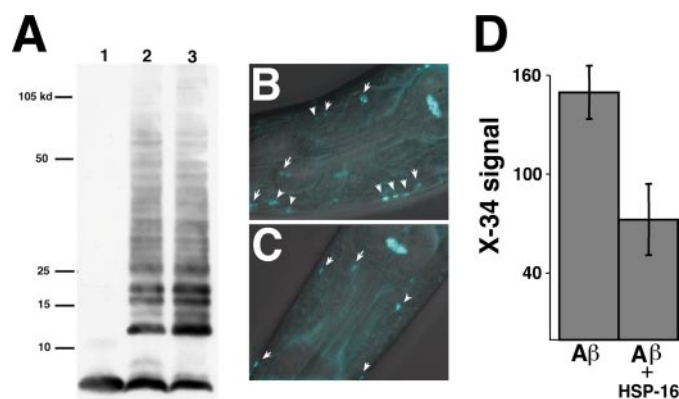


FIGURE 5. HSP-16.2 expression reduces *in vivo* amyloid formation. *A*, anti-A β immunoblot (mAb 6E10). Lane 1, synthetic A β -(1–42) standard; lane 2, total protein from *unc-54/A β* worms (strain CL2006); lane 3, total protein from dual transgenic *unc-54/A β* ; *myo-3/HSP-16.2* worms. Note similar levels of monomeric and multimeric A β species in these strains. *B* and *C*, quantification method to measure β amyloid deposition. Live adult worms ($n = 40$) stained with fluorescent amyloid dye X-34 (5) were imaged, and anterior amyloid deposits (arrows) lying between upper and lower bulbs of the pharynx were identified and fluorescence area and intensity measured using a digital mask. *B*, upper panel, representative *unc-54/A β* worm; *C*, lower panel, representative dual transgenic *unc-54/A β* ; *myo-3/HSP-16.2*. *D*, co-expression of HSP-16.2 significantly reduces detectable β -amyloid deposition. X-34 signal calculated as product of amyloid area and mean signal intensity, arbitrary units. Error bar = S.E.

the accumulation of conformational variants of A β or specific oligomeric species. To determine whether HSP-16.2 altered the A β multimerization pathway leading to amyloid fibril formation, the *myo-3/HSP-16.2* transgene was introduced into strain CL2006. This previously characterized strain constitutively expresses A β -(1–42) in muscle cells, resulting in the formation of intracellular amyloid deposits (3, 5). (Amyloid deposits are not detected in transgenic strains with acute, induced A β expression such as CL4176.) Immunoblot of CL2006 and its *myo-3/HSP-16.2* dual transgenic derivative revealed that the *myo-3/HSP-16.2* transgene did not appreciably change the levels of A β monomer or oligomer species (Fig. 5*A*), as described above for the inducible A β dual transgenic strains. However, quantitation of the *in vivo* amyloid load, using the fluorescent amyloid-specific dye X-34, indicated that co-expression of the *myo-3/HSP-16* did significantly reduce amyloid formation (Fig. 5, *B*, *C*, and *D*).

To investigate directly whether HSP-16.2 can bind to A β and modulate A β oligomerization, *in vitro* experiments were performed with recombinant HSP-16.2 and synthetic A β -(1–42). Samples containing A β -(1–42) oligomers (“globulomers”) were prepared by incubation of A β in Me₂SO, as described previously (34), to mimic the collection of high molecular weight oligomeric A β species detected in the worm transgenic models. The mixed A β species were incubated with biotinylated HSP-16.2, and HSP-16.2-A β complexes were recovered by avidin affinity pulldown. As shown in Fig. 6*A*, A β was co-recovered with HSP-16.2 in this pulldown experiment, with oligomeric species predominating. This preferential binding of HSP-16.2 to A β oligomers *in vitro* recapitulates the preferential co-immunoprecipitation of A β oligomers with HSP-16 in lysates from transgenic worms expressing A β (Fig. 2*A*) (16). To investigate if this HSP-16.2/A β interaction can alter A β oligomerization, HSP-16.2 was co-incubated with A β -(1–42)

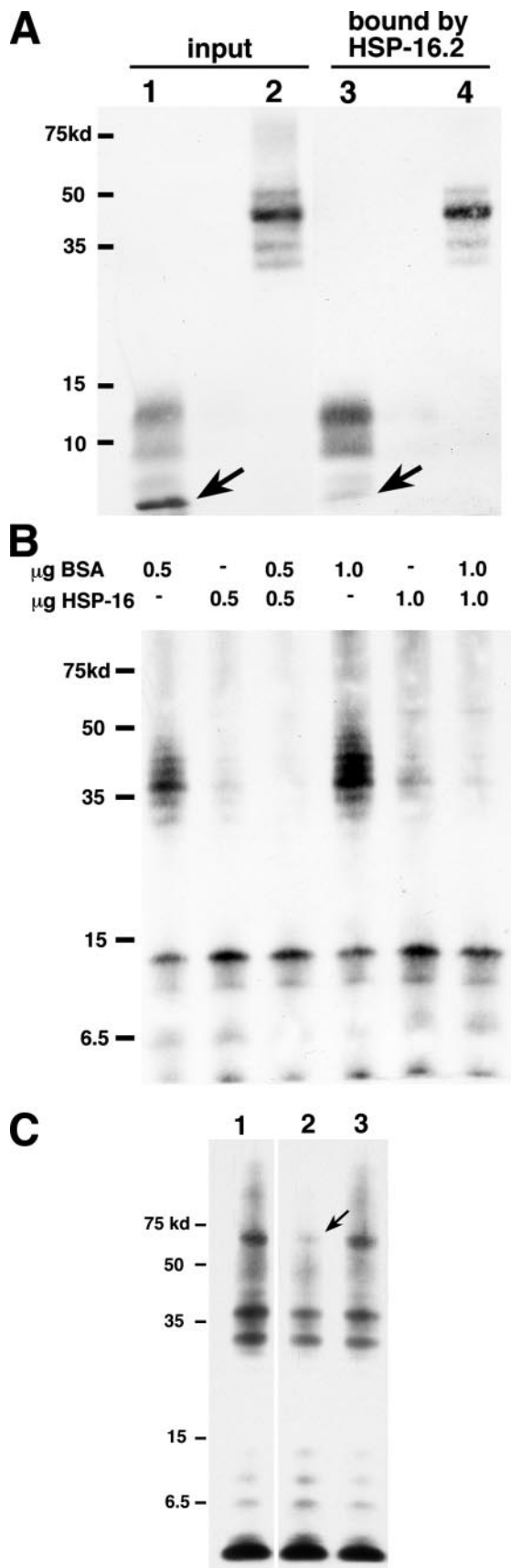


FIGURE 6. **Interaction of HSP-16.2 and A β (1–42) *in vitro*.** A, immunoblot of pull-down of A β oligomers by recombinant HSP-16.2. Preparations of A β (1–42) containing monomeric and low molecular weight oligomers (lane 1,

during the oligomerization incubation. Immunoblot analysis of the oligomeric A β species resulting from these incubations demonstrated that co-incubation with WT HSP-16.2 significantly decreased the formation of higher molecular weight A β species (Fig. 6B). Direct comparison of the activities of WT and R94G recombinant HSP-16.2 in the oligomerization assay indicated that, as predicted from the *in vivo* experiments, the mutant form was less effective than WT in inhibiting A β oligomerization (Fig. 6C).

DISCUSSION

We have demonstrated that overexpression of HSP-16.2, a *C. elegans* chaperone protein homologous to α B crystallin, can suppress toxicity associated with human A β (1–42) in a *C. elegans* AD model. Chaperone expression has not been demonstrated previously to suppress A β toxicity in an *in vivo* model, although the toxicity observed when primary rat hippocampal neurons are transfected with an adenovirus vector driving A β expression is reduced if the neurons are co-transfected with an HSP70-expressing vector (38). HSP70 overexpression has been observed to suppress toxicity in fly (39) and mouse models (40) of polyglutamine repeat diseases. In both these models, HSP70 overexpression suppressed toxicity without altering the nuclear inclusions associated with toxic polyglutamine protein expression. HSP40 (DnaJ) family chaperones have also been found to suppress toxicity in fly polyglutamine repeat disease models (39, 41). HSP70 overexpression has also been observed to suppress α -synuclein toxicity in a fly model of Parkinson disease, again without altering the formation of the Lewy body-like deposits observed in this model (42). These observations are consistent with our results demonstrating that chaperone suppression of A β toxicity occurs without reduction of toxic protein accumulation *per se*.

The formation of HSP-16.2-containing inclusions in transgenic worms overexpressing this protein was unexpected, but perhaps not surprising, given that sHSPs typically function as large oligomers, and avian HSP25 expressed in HeLa cells has also been observed to form inclusions (43). The R120G mutant form of α B-crystallin, associated with desmin-related myopa-

spontaneous oligomers generated in aqueous A β solution) or high molecular weight oligomers (lane 2, oligomers generated by Me₂SO incubation) were mixed with biotinylated recombinant HSP-16.2, and bound complexes were recovered using streptavidin-agarose beads (lane 3, low molecular weight A β input; lane 4, high molecular weight A β input). Note poor recovery of monomeric A β (arrow, lane 3.) The bound portion of this immunoblot (lanes 3 and 4) was exposed for a longer time period than the input half to highlight the preferential recovery of A β oligomers. A β detection was by monoclonal antibody 6E10. B, inhibition of *in vitro* oligomerization by HSP-16.2. Monomeric A β was incubated in Me₂SO as described under "Experimental Procedures" along with control protein (bovine serum albumin, BSA) and/or HSP-16.2. Aliquots of the oligomerization reactions were fractionated after a 6-h incubation. Note that inclusion of HSP-16.2 in the oligomerization reaction strongly reduces the accumulation of higher molecular weight oligomers detected by immunoblot after completion of the oligomerization reaction. C, wild type HSP-16.2 is more efficient at inhibiting A β oligomerization than HSP-16.2 R94G. Monomeric A β was incubated in Me₂SO with 4 μ g of BSA, with or without 0.5 μ g of HSP-16.2 (WT or R94G) for 6 h, diluted 3-fold, and then incubated another 12 h before fractionation. (These conditions were chosen to highlight the differences in the oligomerization inhibition activities of WT and R94G HSP-16.2.) Lane 1, A β + BSA only; lane 2, A β + BSA + WT HSP-16.2; lane 3, A β + BSA + HSP-16.2 R94G. Note that the prominent reduction of an ~70-kDa A β species by WT HSP-16.2 (arrow) is not seen in the reaction containing HSP-16.2 R94G.

thy, has also been reported to form toxic amyloidic oligomers *in vitro* (44). We have not observed HSP-16 inclusions in wild type worms induced to express HSP-16 by heat shock, which may be due to the lower levels of naturally induced HSP-16 and/or the co-induction of other stress proteins that interact with HSP-16. The observation that A β -(1–42), but not the A β single chain dimer, is sequestered into the HSP-16.2 inclusions argues that HSP-16.2 recognition of A β is conformation-dependent and occurs despite the formation of HSP-16.2 inclusions. Similarly, we have also observed that an aggregating form of GFP, but not soluble GFP, is sequestered into HSP-16 inclusions (32). Taken together, these data imply that *in vivo* HSP-16 binding involves the recognition of a conformational motif generally present on some species of aggregation-prone proteins.

We have attempted to complement these overexpression studies by examining the effect of reducing HSP-16.2 expression by RNA interference, which we would predict to enhance the toxicity associated with A β expression. Our results from these experiments have been inconsistent, which we attribute to the multiple *hsp-16* genes present in *C. elegans* and the existence of compensatory cross-regulation between members of this gene family. We have demonstrated previously that RNA interference knockdown of the ER chaperone HSP-3 leads to a compensatory up-regulation of related ER chaperone HSP-4, which effectively mitigates the biological effects of HSP-3 knockdown (45).

How does HSP-16.2 suppress A β toxicity? Given the direct interaction between this chaperone and A β , the simplest models posit that this interaction alters A β metabolism, thereby reducing the amount of toxic A β species. Our results indicate that the overall amount of A β is not reduced by HSP-16.2 overexpression, arguing against the idea that HSP-16.2 promotes degradation of A β . Likewise, the predominant forms of SDS-stable A β oligomers are similarly not detectably changed by HSP-16.2 overexpression. In transgenic worms constitutively expressing A β , HSP-16.2 overexpression does significantly reduce amyloid load. Amyloid deposition does not correlate with toxicity in this *C. elegans* model (46), so this result does not directly explain the reduction in paralysis rate resulting from HSP-16.2 overexpression. We interpret the reduction in amyloid formation as indicative of HSP-16.2 modulating multimerization pathways of A β , possibly leading to changes in the accumulation of a (nonamyloidic) toxic species. (This hypothetical toxic A β species may constitute a minor fraction of all A β , and thus be difficult to detect by immunoblot-based methods.) To investigate directly whether HSP-16.2 can modulate A β oligomerization, we examined the effect of co-incubation of recombinant HSP-16.2 with synthetic A β -(1–42), using an established oligomerization protocol (34). Co-incubation with HSP-16.2 was found to decrease the formation of higher molecular weight A β species, consistent with the proposal that the chaperone activity of HSP-16.2 acts to direct A β along pathways leading to less toxic oligomeric species. This interpretation was further supported by our demonstration that the R94G mutant of HSP-16.2, which shows significantly less protection against A β toxicity *in vivo*, also showed a reduced capacity to inhibit the formation of A β oligomers *in vitro*. Given our current data, we cannot exclude the possibility that HSP-16.2

could also act downstream of the formation of toxic A β species to intervene in the toxic process itself, perhaps by counteracting perturbations of cellular protein folding caused by A β accumulation (47).

The simple *C. elegans* model described in this study does not replicate many aspects of human AD (e.g. formation of extracellular senile plaques or neuronal dysfunction). The rationale for using this model is that it can capture some of the disease-relevant biology that underlies AD and IBM, such as the mechanism(s) by which A β perturbs cell function, and the protective responses of cells to toxic A β accumulation. *C. elegans* does not naturally produce the A β peptide, so the interaction of HSP-16.2 and A β is likely to result from a general function of HSP-16.2 that can influence multimerization/aggregation pathways of potentially toxic proteins. Our results suggest that the HSP-16.2 interaction with A β involves recognition of a conformational epitope associated with A β oligomerization. *In vitro* studies have demonstrated that many proteins can potentially form toxic oligomers (48), suggesting that cells may have a continual need to counteract toxic protein oligomerization. Interestingly, transgenic overexpression of HSP-16 has also been observed to increase the life span in *C. elegans* (7). We speculate that an evolved function of small heat shock proteins may be to bind intermediate multimers that occur during the formation of higher molecular weight oligomers, thus reducing the formation of toxic oligomer species. Small heat shock proteins may therefore play a role in a range of neurodegenerative diseases associated with toxic protein aggregates. If this hypothesis is true, we would predict that risk alleles for some neurodegenerative diseases may be associated with genes encoding small heat shock proteins, and furthermore, diminished small heat shock protein function with age may play a role in the age-dependent onset of these diseases.

Acknowledgments—We thank Michel Leroux for kindly providing the HSP-16.2 expression plasmid, Justin Springett for media preparation, and Gretchen Stein and Maria McClure for careful reading of this manuscript. Some nematode strains were provided by the *Caenorhabditis Genetics Center*, funded by the National Institutes of Health National Center for Research Resources. The JLA20 monoclonal antibody was obtained from the Developmental Studies Hybridoma Bank developed under the auspices of the NICHD, National Institutes of Health.

REFERENCES

- Hardy, J., and Selkoe, D. J. (2002) *Science* **297**, 353–356
- Askanas, V., Engel, W. K., and Alvarez, R. B. (1992) *Am. J. Pathol.* **141**, 31–36
- Link, C. D. (1995) *Proc. Natl. Acad. Sci. U. S. A.* **92**, 9368–9372
- Link, C. D. (2006) *Exp. Gerontol.* **41**, 1007–1013
- Link, C. D., Johnson, C. J., Fonte, V., Paupard, M., Hall, D. H., Styren, S., Mathis, C. A., and Klunk, W. E. (2001) *Neurobiol. Aging* **22**, 217–226
- Fonte, V., Kapulkin, V., Taft, A., Fluet, A., Friedman, D., and Link, C. D. (2002) *Proc. Natl. Acad. Sci. U. S. A.* **99**, 9439–9444
- Walker, G. A., and Lithgow, G. J. (2003) *Aging Cell* **2**, 131–139
- Florez-McClure, M. L., Hohsfield, L. A., Fonte, G., Bealor, M. T., and Link, C. D. (2007) *Autophagy* **3**, 569–580
- Kitazawa, M., Green, K. N., Caccamo, A., and LaFerla, F. M. (2006) *Am. J. Pathol.* **168**, 1986–1997
- Moussa, C. E., Fu, Q., Kumar, P., Shtifman, A., Lopez, J. R., Allen, P. D.,

- LaFerla, F., Weinberg, D., Magrane, J., Aprahamian, T., Walsh, K., Rosen, K. M., and Querfurth, H. W. (2006) *FASEB J.* **20**, 2165–2167
11. Gouras, G. K., Tsai, J., Naslund, J., Vincent, B., Edgar, M., Checler, F., Greenfield, J. P., Haroutunian, V., Buxbaum, J. D., Xu, H., Greengard, P., and Relkin, N. R. (2000) *Am. J. Pathol.* **156**, 15–20
 12. Oddo, S., Caccamo, A., Shepherd, J. D., Murphy, M. P., Golde, T. E., Kaye, R., Metherate, R., Mattson, M. P., Akbari, Y., and LaFerla, F. M. (2003) *Neuron* **39**, 409–421
 13. Cohen, E., Bieschke, J., Perciavalle, R. M., Kelly, J. W., and Dillin, A. (2006) *Science* **313**, 1604–1610
 14. Link, C. D., Cypser, J. R., Johnson, C. J., and Johnson, T. E. (1999) *Cell Stress Chaperones* **4**, 235–242
 15. Link, C. D., Taft, A., Kapulkin, V., Duke, K., Kim, S., Fei, Q., Wood, D. E., and Sahagan, B. G. (2003) *Neurobiol. Aging* **24**, 397–413
 16. Fonte, V., Kapulkin, V., Taft, A., Fluet, A., Friedman, D., and Link, C. D. (2002) *Proc. Natl. Acad. Sci. U. S. A.* **99**, 9439–9444
 17. Leroux, M. R., Melki, R., Gordon, B., Batelier, G., and Candido, E. P. (1997) *J. Biol. Chem.* **272**, 24646–24656
 18. Taylor, R. P., and Benjamin, I. J. (2005) *J. Mol. Cell. Cardiol.* **38**, 433–444
 19. Shinohara, H., Inaguma, Y., Goto, S., Inagaki, T., and Kato, K. (1993) *J. Neurol. Sci.* **119**, 203–208
 20. Renkawek, K., Voorter, C. E., Bosman, G. J., van Workum, F. P., and de Jong, W. W. (1994) *Acta Neuropathol.* **87**, 155–160
 21. Yoo, B. C., Kim, S. H., Cairns, N., Fountoulakis, M., and Lubec, G. (2001) *Biochem. Biophys. Res. Commun.* **280**, 249–258
 22. Goldstein, L. E., Muffat, J. A., Cherny, R. A., Moir, R. D., Ericsson, M. H., Huang, X., Mavros, C., Coccia, J. A., Faget, K. Y., Fitch, K. A., Masters, C. L., Tanzi, R. E., Chylack, L. T., Jr., and Bush, A. I. (2003) *Lancet* **361**, 1258–1265
 23. Banwell, B. L., and Engel, A. G. (2000) *Neurology* **54**, 1033–1041
 24. Wilhelmus, M. M., Boelens, W. C., Otte-Holler, I., Kamps, B., de Waal, R. M., and Verbeek, M. M. (2006) *Brain Res.* **1089**, 67–78
 25. Wilhelmus, M. M., Boelens, W. C., Otte-Holler, I., Kamps, B., Kusters, B., Maat-Schieman, M. L., de Waal, R. M., and Verbeek, M. M. (2006) *Acta Neuropathol.* **111**, 139–149
 26. Stege, G. J., Renkawek, K., Overkamp, P. S., Verschuure, P., van Rijk, A. F., Reijnen-Aalbers, A., Boelens, W. C., Bosman, G. J., and de Jong, W. W. (1999) *Biochem. Biophys. Res. Commun.* **262**, 152–156
 27. Liang, J. J. (2000) *FEBS Lett.* **484**, 98–101
 28. Raman, B., Ban, T., Sakai, M., Pasta, S. Y., Ramakrishna, T., Naiki, H., Goto, Y., and Rao, ChM. (2005) *Biochem. J.* **392**, 573–581
 29. Santhoshkumar, P., and Sharma, K. K. (2004) *Mol. Cell. Biochem.* **267**, 147–155
 30. Lee, S., Carson, K., Rice-Ficht, A., and Good, T. (2005) *Protein Sci.* **14**, 593–601
 31. Kudva, Y. C., Hiddinga, H. J., Butler, P. C., Mueske, C. S., and Eberhardt, N. L. (1997) *FEBS Lett.* **416**, 117–121
 32. Link, C. D., Fonte, V., Hiester, B., Yerg, J., Ferguson, J., Csontos, S., Silverman, M. A., and Stein, G. H. (2006) *J. Biol. Chem.* **281**, 1808–1816
 33. Dahl, R., and Staehelin, L. A. (1989) *J. Electron Microsc. Technol.* **13**, 165–174
 34. Barghorn, S., Nimmrich, V., Striebing, A., Krantz, C., Keller, P., Janson, B., Bahr, M., Schmidt, M., Bitner, R. S., Harlan, J., Barlow, E., Ebert, U., and Hillen, H. (2005) *J. Neurochem.* **95**, 834–847
 35. Bova, M. P., Yaron, O., Huang, Q., Ding, L., Haley, D. A., Stewart, P. L., and Horwitz, J. (1999) *Proc. Natl. Acad. Sci. U. S. A.* **96**, 6137–6142
 36. Chavez Zobel, A. T., Loranger, A., Marceau, N., Theriault, J. R., Lambert, H., and Landry, J. (2003) *Hum. Mol. Genet.* **12**, 1609–1620
 37. Fay, D. S., Fluet, A., Johnson, C. J., and Link, C. D. (1998) *J. Neurochem.* **71**, 1616–1625
 38. Magrane, J., Smith, R. C., Walsh, K., and Querfurth, H. W. (2004) *J. Neurosci.* **24**, 1700–1706
 39. Chan, H. Y., Warrick, J. M., Gray-Board, G. L., Paulson, H. L., and Bonini, N. M. (2000) *Hum. Mol. Genet.* **9**, 2811–2820
 40. Cummings, C. J., Sun, Y., Opal, P., Antalffy, B., Mestril, R., Orr, H. T., Dillmann, W. H., and Zoghbi, H. Y. (2001) *Hum. Mol. Genet.* **10**, 1511–1518
 41. Kazemi-Esfarjani, P., and Benzer, S. (2000) *Science* **287**, 1837–1840
 42. Auluck, P. K., Chan, H. Y., Trojanowski, J. Q., Lee, V. M., and Bonini, N. M. (2002) *Science* **295**, 865–868
 43. Katoh, Y., Fujimoto, M., Nakamura, K., Inouye, S., Sugahara, K., Izu, H., and Nakai, A. (2004) *FEBS Lett.* **565**, 28–32
 44. Sanbe, A., Yamauchi, J., Miyamoto, Y., Fujiwara, Y., Murabe, M., and Tanoue, A. (2007) *J. Biol. Chem.* **282**, 555–563
 45. Kapulkin, V., Hiester, B. G., and Link, C. D. (2005) *FEBS Lett.* **579**, 3063–3068
 46. Drake, J., Link, C. D., and Butterfield, D. A. (2003) *Neurobiol. Aging* **24**, 415–420
 47. Gidalevitz, T., Ben-Zvi, A., Ho, K. H., Brignull, H. R., and Morimoto, R. I. (2006) *Science* **311**, 1471–1474
 48. Glabe, C. G., and Kaye, R. (2006) *Neurology* **66**, S74–S78

Suppression of *in Vivo* β -Amyloid Peptide Toxicity by Overexpression of the HSP-16.2 Small Chaperone Protein

Virginia Fonte, D. Randal Kipp, John Yerg III, David Merin, Margaret Forrestal, Eileen Wagner, Christine M. Roberts and Christopher D. Link

J. Biol. Chem. 2008, 283:784-791.

doi: 10.1074/jbc.M703339200 originally published online November 9, 2007

Access the most updated version of this article at doi: [10.1074/jbc.M703339200](https://doi.org/10.1074/jbc.M703339200)

Alerts:

- [When this article is cited](#)
- [When a correction for this article is posted](#)

[Click here](#) to choose from all of JBC's e-mail alerts

This article cites 48 references, 19 of which can be accessed free at <http://www.jbc.org/content/283/2/784.full.html#ref-list-1>